International Journal of Power Electronics and Drive System (IJPEDS)
Vol. 17, No. 1, March 2026, pp. 317~334
ISSN: 2088-8694, DOI: 10.11591/ijpeds.v17.i1.pp317-334

Grid-tied photovoltaic system MPPT algorithms performance: comparative analysis

Louis Nicase Nguefack, Kayode Timothy Akindeji, Abayomi A. Adebiyi
Department of Electrical Power Engineering, Faculty of Engineering and the Built Environment,
Durban University of Technology, Durban, South Africa

Article Info

Article history:

Received Jan 23, 2025
Revised Dec 23, 2025
Accepted Jan 23, 2026

Keywords:

Artificial neural network
Fuzzy logic controller
Incremental conductance
Maximum power point
Perturbation and observation

ABSTRACT

Between 2015 and 2024, global solar photovoltaic (PV) capacity rose significantly from 223.204 GW to 1624 GW, contributing to the reduction of greenhouse gas emissions associated with fossil-fuel-based power generation. Solar PV is recognized for its environmental benefits and is increasingly seen as a viable alternative for a long-term sustainable energy supply. However, the power output of PV systems is highly dependent on atmospheric conditions, particularly solar irradiation and temperature, which can cause fluctuations and reduce overall efficiency. To address this, maximum power point tracking (MPPT) techniques are employed to optimize energy extraction under varying environmental conditions. This study presents a comparative analysis of four MPPT algorithms, perturb-and-observe (P&O), incremental conductance (InC), fuzzy logic control (FLC), and artificial neural network (ANN) for grid-tied PV systems using MATLAB/Simulink. Each algorithm was evaluated under dynamic conditions to determine its tracking efficiency and responsiveness. The results show that while conventional methods like P&O and InC are simpler, they are less effective under rapidly changing conditions. FLC demonstrates faster convergence but requires greater computational resources. The intelligent controllers demonstrated superior performance: FLC achieved the highest power output of 1.019×10^{6} W with a corresponding voltage of 1.422×10^{4} V, while the ANN algorithm followed closely with 9.650×10^{5} W and 1.200×10^{4} V, respectively. The comparative insights gained from this analysis offer practical guidance for selecting MPPT controllers in real-world solar energy applications.

Corresponding Author:

Abayomi A. Adebiyi
Department of Electrical Power Engineering, Faculty of Engineering and the Built Environment
Durban University of Technology
Durban, South Africa
Email: abayomia@dut.ac.za

1. INTRODUCTION

Photovoltaic (PV) cells are devices that detect electromagnetic radiation and dissipate current or voltage, or both, in response to the concentration of solar insolation. Its application has gone exponential, as presented in Figure 1. The approach to harnessing the maximum potential of solar energy is termed maximum power point tracking (MPPT). An MPPT is a type of electronic DC to DC regulator that maximizes compatibility across the load and the solar PV array. The main application and merits of MPPT in solar power system generation are to maximize the capability and energy of solar cells [1]. Escalating global energy needs are driving a rapid rise in the consumption of fossil fuels, resulting in detrimental

environmental effects like global warming, acid rain, and ozone layer depletion [1]. To safeguard the Earth's ecological balance, it is imperative to diversify energy resources and mitigate the adverse impacts associated with fossil fuel technologies. Moreover, the impending challenges of soaring fuel costs and diminishing fossil fuel reserves may have adverse economic and political consequences for numerous nations in the coming years. To ensure sustainable development, enhancing energy efficiency and maximizing the utilization of renewable energy sources (RES) are of paramount importance [1]-[4]. One potential solution to address this crisis is the utilization of RES. Amongst these, solar energy holds great promise and is expected to witness significant growth in its market share. PV cells are a viable method for harnessing solar energy. However, a challenge with the solar system is its intermittent nature, as the times of maximum solar insolation rarely align with energy demand. Hence, it is logical to store the PV energy generated during periods of high sunlight not only to sustain power supply during low-insolation times or cloudy periods but also to ensure a continuous electric power output [5]. The global PV rooftop and utility-scale segments' growth is depicted in Figure 1.

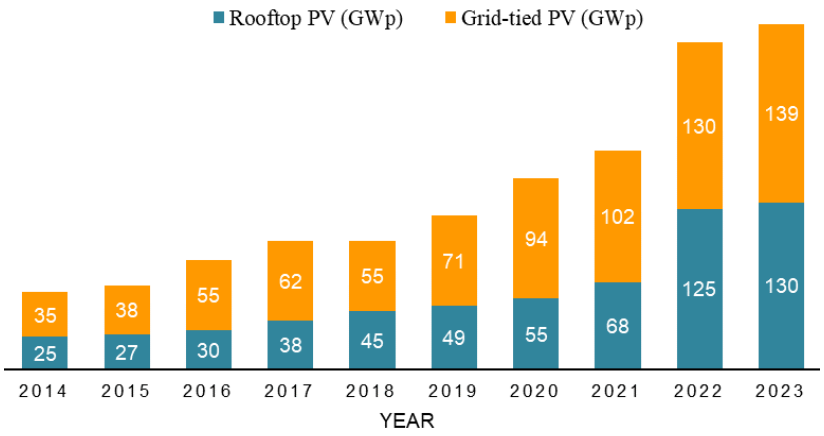

Figure 1. Global PV rooftop and utility-scale segments growth [2]

One of the primary challenges facing PV systems is operating at maximum power under all environmental conditions, including temperature fluctuations, shifting sunlight, shade conditions, and module ageing. To address these issues, an efficient algorithm called maximum power point tracking (MPPT) has been developed [6], which will increase system efficiency and lower costs [7]. Many research studies offer various methods to attain MPPT. As they are simple to use and reasonably priced, perturb and observe (P&O), and incremental conductance (InC) are a few of the traditional MPPT methods that have been extensively utilized for tracking the MPP [8].

Additionally, oscillations near MPP are caused by a specific predilection. The poor tracking speed and strong oscillations near MPP are problems with these methods [9]. Numerous research studies have sought to resolve this issue by introducing artificial intelligence methodologies and optimization strategies, such as fuzzy logic controllers (FLC) [10]-[17]. While the Chimp optimization algorithm does not require a mathematical model or technical knowledge of the exact mode of operation, it can deal with the nonlinear properties [18]. In several applications, artificial neural network (ANN) techniques are widely used to handle nonlinearity [19]. Additionally, the best MPPT solution is explored by the application of machine learning (ML) [20]. Their effectiveness is largely reliant on thorough training, which typically requires a significant amount of processing power and time to complete [21].

Recent research has shown a particular interest in bio-inspired MPPT algorithms, which have produced superior outcomes than evolutionary MPPT controllers in terms of increased precision and speed. For global point tracking, this study used artificial neural networks and fuzzy logic control. These methods tracked the global point satisfactorily in both standard sun radiation and partially shaded conditions. However, these methods need intricate calculations.

This work proposes a comprehensive comparative analysis of MPPT algorithms within a grid-tied photovoltaic system context. Unlike previous studies that focus only on standalone PV systems or simplified irradiance profiles, this study evaluates the algorithms' tracking behavior under realistic grid-tied constraints. The specific goals include: i) Implementing four widely used MPPT techniques (Perturb and Observe, incremental conductance, fuzzy logic, and the artificial neural network) under identical test conditions;

ii) Assessing their tracking efficiency, convergence time, voltage ripple, and output power stability; and iii) Analyzing their suitability for integration with grid-tied inverter systems. The study introduces a unified testing framework using MATLAB/Simulink, which allows direct and fair comparison. Findings show that while P&O is simple, it suffers under rapidly changing conditions, whereas fuzzy logic-controlled MPPT offers faster convergence but is computationally intensive, providing actionable insights for real-world MPPT controller deployment.

This work is structured into five main sections for clarity and flow: i) Section 1 introduces the study, outlining the problem, objectives, and significance of the research; ii) Section 2 covers the electrical modelling and characteristics of the photovoltaic (PV) system, explaining the methodology used in the study; iii) In section 3, the proposed MPPT algorithms are described in detail, highlighting their working principles and relevance; iv) Section 4 presents the simulation results, including a thorough analysis and comparison of the performance of the proposed techniques; and v) Finally, section 5 concludes the paper by summarizing the key findings and their implications.

2. METHOD

This study appraises the appropriate literature on state-of-the-art PV technology and other related IEEE standards in the design of power systems. A test system was used, and it was modelled and simulated in MATLAB/Simulink software. The approach includes the modelling of 25 panels in series and 20 parallel modules, respectively, with a total of 775 kW required, and the mathematical modelling of the PV system using several MPPT algorithms to support the research objectives. Moreover, a sensitivity study was performed to differentiate the worth of each MPPT algorithm, respectively, to be implemented in MATLAB/Simulink software. The features of semiconductor p-n diodes and solar cells are very similar. One popular model used to represent the equivalent electrical circuit of a solar cell is a single-diode model, as shown in Figure 2 [1].

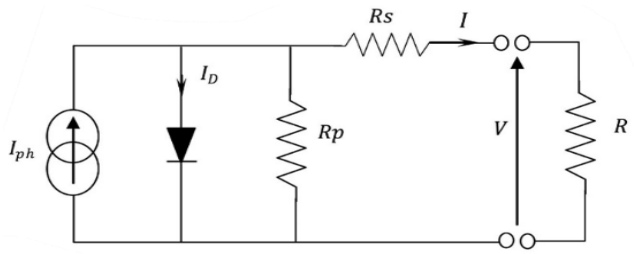

Figure 2. Equivalent solar cell circuit of a single-diode model [1]

In the context of the PV cell, the output current and output voltage are denoted as *I* and *V*, respectively. The diode's reverse saturation current is represented by I_O, while the diode ideality factor is denoted as a. Additionally, the symbols R_P and R_S denote parallel and series resistance, respectively.

$$I = I_{ph} - I_O \left[exp\left(\frac{V+I\times R_S}{a\times V_{sh}}\right) - 1\right] - \frac{V+I\times R_S}{R_p} \quad (1)$$

$$I_{ph} = \left[I_{SC\_STC} + K_a(T - T_{STC})\right]\frac{G}{G_{STC}} \quad (2)$$

Where the short-circuit current at standard test conditions (STC) is represented by $Isc_{\_STC}$. The cell temperature at STC is indicated by T_{STC} (25 °C), G (W/m^2) representing the insolation incident on the PV cell surface. The insolation level at STC is denoted by G_{STC} (1000 W/m^2), and the short circuit current coefficient, or K_a, is usually given by the cell manufacturer. Moreover, (2) explains how temperature affects the saturation current I_O [3]. The open circuit voltage under standard test circumstances (STC) is represented by V_{OC_STC} in the context provided.

$$I_O = \frac{I_{SC_{STC}} + K_a(T - T_{STC})}{exp\left[\left(V_{OC_{STC}} + K_b(T - T_{STC})\right)/a\times V_{th}\right] - 1} \quad (3)$$

Numerous DC-DC converters were invented, including buck, cuk, and boost converters. Considering its outstanding efficiency, the boost converter is the most popular choice among these for PV-generated systems [1]. The primary cause is that, as a loss power equation shows, it can provide and control an output voltage that is higher than the input voltage while maintaining a low output current. The DC-DC boost converter's key component is a transistor that controls the amplified processing via a controller. Transistors such as the insulated gate bipolar transistor (IGBT), bipolar junction transistor (BJT), and metal oxide semiconductor field effect transistor (MOSFET) are frequently utilized in DC-DC converters. The output voltage is continuously higher than the input voltage due to the boost converter. The circuit topology of the boost converter is shown in Figure 3. Tables 1 and 2 present the converter parameters and network and inverter parameters used in this study.

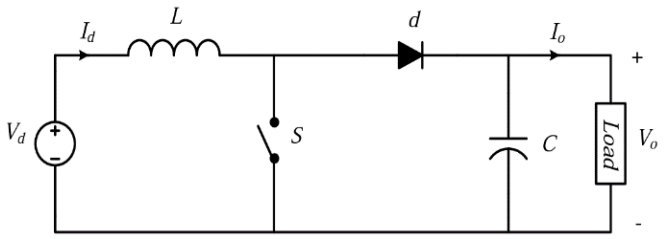

Figure 3. Boost converter circuit topology [1]

Table 1. Boost converter parameters

Description	Value
Switching frequency (Hz)	5000
Inductor resistance	0.1 Ω
Inductance	$100e^{-3}$ H
Capacitor resistance	0.1 Ω
Capacitance	$50e^{-6}$ F
Load	150 Ω

Table 2. Existing network and inverter parameters

Description	Value	Description	Value
Breaker resistance (Ohm)	0.01	Source inductance (H)	$16.58e^{-3}$
Snubber resistance (Ohm)	$1e^{6}$	Base voltage (Vrms) Ph-Ph	$25e^{3}$
Snubber capacitance Cs (F)	Inf	Nominal phase-to-phase voltage Vn (Vrms)	380
Phase-to-phase voltage (Vrms)	380	Nominal frequency fn (HZ)	50
Frequency (HZ)	50	Active power P (W)	$10e^{3}$
Source resistance (Ohm)	0.8929		

When the switch S is turned on, the diode D becomes reverse-biased, meaning it no longer conducts current. As a result, the inductor L is effectively disconnected from the output side and instead becomes part of a closed loop with the voltage source. This causes the current through the inductor to increase linearly due to the applied input voltage, since the inductor resists changes in current by storing energy in its magnetic field. During this interval, the output stage is isolated from the input, and the load receives power solely from the discharge of the output capacitor C, which temporarily maintains the output voltage and supplies current to the load.

Figure 4 illustrates the behavior of the inductor current in continuous conduction mode (CCM), where the current flowing through the inductor remains nonzero throughout the entire switching cycle. In this mode, the inductor current remains positive (i.e., $I_L(t) > 0$) at all times, ensuring continuous energy transfer and improved efficiency in power delivery. Under steady-state conditions in CCM, the duty cycle D, which is the ratio of the switch-on time to the total switching period, can be calculated using (4).

$$D = 1 - \frac{V_d}{V_o} \tag{4}$$

Where: V_d is the input voltage, *Vo* is the converter's output voltage, and D is the duty ratio.

The output voltage V_O of the converter increases proportionally with the duty ratio *D*, as indicated by (4). This relationship shows that by adjusting the amount of time the switch remains on during each switching cycle, the average voltage delivered to the load can be effectively controlled. As the duty ratio increases, the converter transfers more energy to the output, resulting in a higher output voltage. However, changing the duty ratio not only affects the output voltage but also influences the behaviour of both the input and output currents of the converter. These variations can impact the overall stability and efficiency of the system, especially in continuous conduction mode (CCM), where the inductor current never drops to zero. To ensure smooth and stable operation in this mode, it is essential to properly design the passive components, namely, the inductor and capacitor used in the converter.

The (5) is used to calculate the value of the inductor L required to limit the current ripple ΔI_L and maintain continuous conduction (5).

$$L = \frac{V_d D}{2\Delta I_L f_p} \tag{5}$$

Here, V_d is the input voltage, D is the duty ratio, ΔI_L is the peak-to-peak inductor current ripple, and f_p is the switching frequency. The (6) provides the required value for the output capacitor C, which smooths the output voltage and reduces the voltage ripple ΔV_O (6).

$$C = \frac{I_O D}{\Delta V_O f_p} \tag{6}$$

Where I_O is the output current, ΔV_O is the allowable output voltage ripple, and f_p is the switching frequency. The proper selection of these components is crucial for achieving the desired performance, minimizing losses, and ensuring the reliable operation of the converter in CCM.

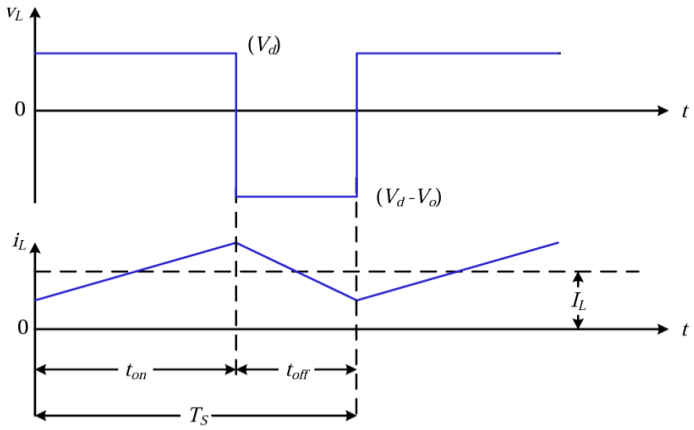

Figure 4. Boost converter voltage and current waveform in continuous conduction operation [1]

3. MAXIMUM POWER POINT TRACKING (MPPT)

In the ever-advancing field of solar energy technology, maximum power point tracking (MPPT) plays a vital role in enhancing the efficiency and performance of PV systems. As solar panels are subject to constantly changing environmental factors, such as irradiance, temperature, and shading, the electrical characteristics of these panels fluctuate. MPPT is a power electronic device integrated with intelligent control algorithms that dynamically track and operate the PV system at its optimal point, known as the maximum power point (MPP). This capability ensures that, regardless of varying conditions, the maximum possible power is extracted from the solar array and delivered to the load with the highest possible efficiency [1].

Traditionally, MPPT methods have relied on algorithmic techniques designed to adjust the operating voltage or current of the PV modules in response to observed changes in power output. Among these, the perturb and observe (P&O) method and the incremental conductance (InC) technique have been the most widely adopted. The P&O method operates by incrementally adjusting the voltage and observing the change in power; if the power increases, the algorithm continues in the same direction; otherwise, it reverses. In contrast, the InC method determines the MPP based on the slope of the power-voltage curve, offering faster and more precise tracking under rapidly changing conditions. Despite their effectiveness, these methods often struggle with tracking delays, oscillations around the MPP, and suboptimal performance during transient environmental events like fast cloud movement or partial shading. To overcome these limitations, this research and development in MPPT have shifted toward intelligent, adaptive techniques rooted in artificial intelligence and soft computing. Artificial neural networks (ANNs) and fuzzy logic controllers (FLCs) are considered at the forefront of this innovation. ANN-based MPPT systems are capable of learning from historical and real-time data, allowing them to predict and respond to changing conditions with a high degree of accuracy. Meanwhile, fuzzy logic provides a rule-based yet flexible approach to handle uncertainties in input parameters, emulating human reasoning to make decisions where precise mathematical models are insufficient. These intelligent methods offer improved tracking speed, reduced oscillations around the MPP, and better adaptability in complex scenarios, making them highly effective in modern PV applications [22].

However, the advancement in MPPT strategies also introduces new challenges. The selection of an MPPT technique must consider multiple practical factors such as computational complexity, response time, implementation cost, and hardware compatibility. While traditional methods are simpler and easier to implement on low-cost microcontrollers, intelligent algorithms often require more sophisticated processors and greater memory, which can increase the overall system cost. Consequently, the choice between classical and advanced MPPT methods depends largely on the specific requirements of the PV application, whether it prioritizes cost-effectiveness, precision, or scalability. Looking ahead, the future of MPPT lies in the development of hybrid and self-adaptive systems that combine the strengths of multiple techniques. Integration with IoT platforms, real-time weather data, and edge computing is expected to enhance the predictive capabilities of MPPT systems, transforming them from reactive controllers into proactive decision-makers. As solar energy continues to scale globally, MPPT will remain a crucial enabler, evolving from a mere efficiency tool into a basis of smart, responsive, and high-performing energy systems [23], [24].

3.1. Perturbation and observation MPPT

The perturbation and observation (P&O) method remains one of the most foundational and widely implemented strategies in the domain of MPPT. Its continued popularity in both academic research and commercial applications stems from a combination of technical simplicity, cost-effectiveness, and ease of real-time implementation. Despite the emergence of more advanced and intelligent tracking algorithms, P&O still holds a central position in MPPT literature and serves as a benchmark for evaluating newer techniques. At the core of the P&O method lies a deceptively simple logic: Perturb the operating voltage or current of the PV system slightly and observe the effect on output power. If the power increases, the perturbation continues in the same direction; if it decreases, the direction is reversed. This trial-and-error approach enables the algorithm to gradually converge on the maximum power point (MPP), where the output power is at its peak for the given environmental conditions. This algorithm can be visualized through a control loop that operates continuously, measuring the current and voltage output of the PV module and making incremental adjustments to the duty cycle of the associated DC-DC converter. A typical flowchart of this decision-making process, such as the one shown in Figure 5, highlights its straightforward logic structure. Since it does not rely on complex mathematical models or extensive datasets, P&O is highly adaptable and can be deployed on inexpensive microcontrollers with limited processing power [25].

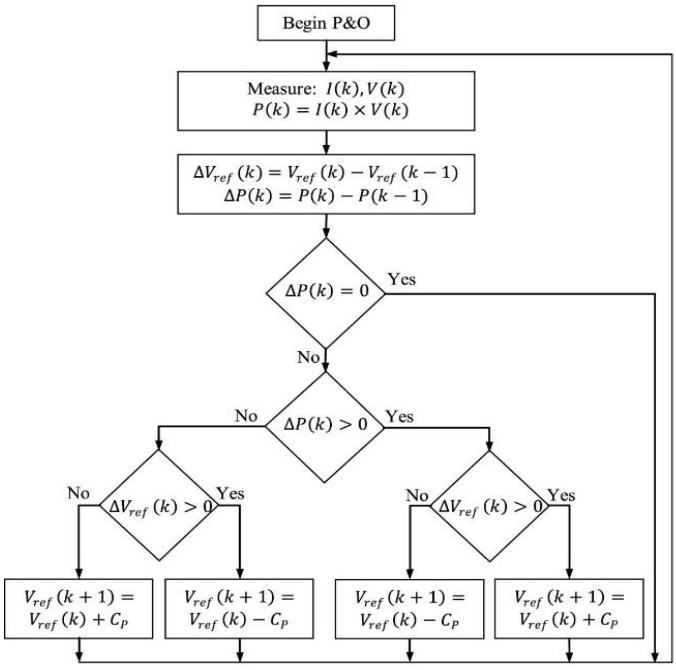

Figure 5. P&O algorithm flowchart [1]

However, the simplicity of the P&O method is both its strength and its limitation. Under steady-state conditions, it performs well and maintains the operating point close to the MPP. Yet, in rapidly

changing environments, such as when clouds pass over a solar array, it may struggle to distinguish whether changes in output power are due to perturbations or external factors. This can lead to oscillations around the MPP or misdirection in the tracking process. Despite this, its low computational overhead and minimal hardware requirements make it an attractive solution for small to medium-scale PV systems, especially in cost-sensitive applications. Remarkably, the principles of the P&O method have served as the blueprint for more sophisticated hybrid and adaptive algorithms. Many researchers have sought to enhance its performance by integrating it with techniques such as fuzzy logic, neural networks, or variable step-size adjustments. These improvements aim to retain the simplicity of P&O while addressing its responsiveness and stability under dynamic conditions. In this sense, the P&O method is not just a basic MPPT technique; it is a catalyst for innovation, a platform upon which the next generation of smart, responsive, and adaptive MPPT strategies continues to be built [26].

3.2. Incremental conductance MPPT

The incremental conductance (InC) method represents a more analytical and mathematically grounded approach to MPPT in PV systems. Its development emerged as a response to the limitations of simpler methods, such as perturbation and observation (P&O), particularly in terms of precision and adaptability to rapidly fluctuating environmental conditions. The InC algorithm is based on a critical insight into the power-voltage (P–V) characteristics of a photovoltaic array. Specifically, it exploits the fact that the derivative of power with respect to voltage, dP/dV, equals zero at the maximum power point (MPP). This principle allows the MPPT controller to determine whether the system has reached the MPP, or whether it should increase or decrease the operating voltage to move closer to it. Unlike perturbation-based techniques that rely on iterative observation, InC calculates this derivative explicitly, using the PV array's real-time output current (I) and voltage (V) data [27]. At the maximum power point, the incremental conductance (dI/dV) and the instantaneous conductance (I/V) are equal, leading to the condition in (7).

$$\frac{dP}{dV} = \frac{d(V \times I)}{dV} = 1 + V\frac{dI}{dV} \rightarrow \frac{1}{V} \times \frac{dP}{dV} = \frac{1}{V} + \frac{dP}{dV} \tag{7}$$

This equality forms the decision-making core of the InC algorithm. If the incremental conductance is greater than the negative of the instantaneous conductance, the operating point lies to the left of the MPP, and the voltage must be increased. Conversely, if the incremental conductance is less, the operating point lies to the right of the MPP, and the voltage must be decreased. Only when the two are equal does the algorithm confirm that the MPP has been located. An algorithmic implementation of this process, illustrated in Figure 6 highlights its systematic nature and responsiveness to dynamic conditions.

The InC method offers a distinct advantage in grid-tied systems, where precision and real-time adaptability are paramount. As it avoids unnecessary oscillations around the MPP and makes informed voltage adjustments based on slope analysis, it enables more stable and efficient operation, particularly under conditions of rapid irradiance fluctuation or partial shading, where other methods often falter. The (8) through (10) provide the logic foundation for the directional decision-making within the InC algorithm. By evaluating the relationship between dI/dV and I/V in real time, the MPPT controller can accurately determine whether to increase, decrease, or maintain the PV operating voltage, ensuring consistent and efficient tracking of the MPP even under rapidly changing environmental conditions [28].

$$\frac{dP}{dV} = 0 \quad if \ \frac{dI}{dV} > -\frac{1}{V}, \ (left \ of \ MPP) \tag{8}$$

$$\frac{dP}{dV} = 0 \quad if \ \frac{dI}{dV} = -\frac{1}{V}, \ (at \ MPP) \tag{9}$$

$$\frac{dP}{dV} = 0 \quad if \ \frac{dI}{dV} < -\frac{1}{V}, \ (right \ of \ MPP) \tag{10}$$

Moreover, due to its deterministic control logic, InC is well-suited for integration into digital controllers and microprocessors used in modern power electronic converters. While it may require slightly more computational resources than P&O, its increased accuracy and tracking stability make it a preferred choice in many high-performance grid-tied PV applications. As a result, the incremental conductance method is not just an alternative to simpler MPPT algorithms, it is a sophisticated strategy that embodies the balance between mathematical rigor, algorithmic precision, and practical performance, and continues to serve as a benchmark in comparative studies of MPPT methods for grid-tied photovoltaic systems [29]. This method measures the PV array's operating voltage (V) and current (I) using two sensors. The (11) and (12) can be used to digitally compute the incremental changes (dV and dI) of the PV array's output current (I) and voltage (V) by sampling these values at successive time intervals (k-1) and (k) [2].

$$dV(k) = V(k) - V(k-1) \tag{11}$$

$$dI(k) = I(k) - I(k-1) \tag{12}$$

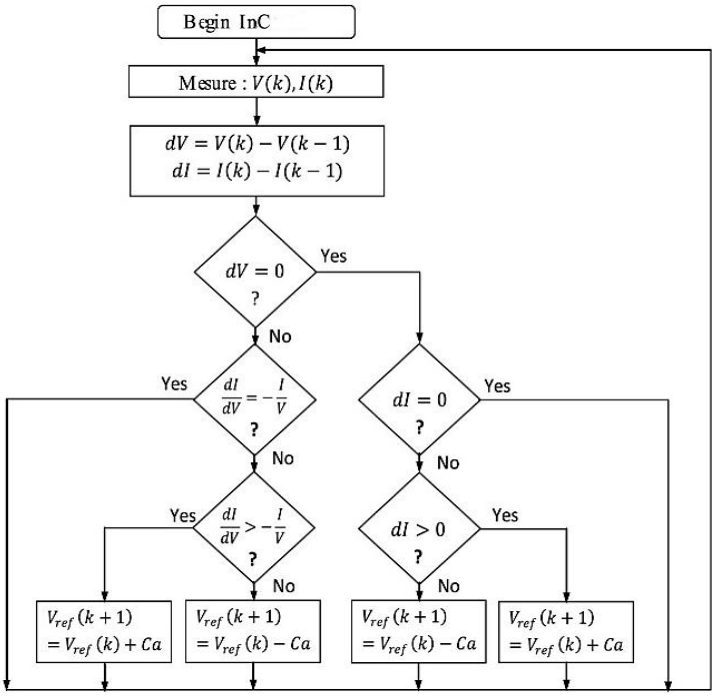

Figure 6. InC MPPT flowchart [1]

3.3. Artificial neural network controlled MPPT

As the demand for smarter, more responsive, and adaptive renewable energy systems increases, Artificial neural networks (ANNs) have emerged as a transformative approach in the development of maximum power point tracking (MPPT) algorithms. Representing a branch of artificial intelligence, ANN-based MPPT strategies offer distinct advantages over traditional techniques, particularly in dynamic and unpredictable environmental conditions. Conventional MPPT algorithms, such as perturbation and observation (P&O) and incremental conductance (InC), while effective in steady-state conditions, often suffer from delayed convergence and suboptimal performance under rapid variations in solar irradiance and temperature. These shortcomings can result in oscillations near the maximum power point (MPP) or failure to track it altogether. In contrast, ANN-based MPPT overcomes these limitations through a data-driven, adaptive learning approach capable of generalizing complex, nonlinear relationships between environmental variables and the system's power output. The core structure of an ANN-controlled MPPT system is illustrated in Figure 7. This configuration typically employs solar irradiance and cell temperature as input variables to the neural network. The network is trained to map these inputs to a corresponding duty ratio for the DC-DC converter, which adjusts the operating point of the photovoltaic (PV) array to match the MPP in real time. This training process utilizes supervised learning techniques, wherein the ANN is presented with multiple scenarios of solar and thermal conditions, and the corresponding optimal duty ratios are determined using known MPP data [30].

One of the most effective training algorithms for this application is the Levenberg-Marquardt backpropagation algorithm, known for its fast convergence and high accuracy in function approximation. During training, the ANN optimizes its internal parameters known as weights through iterative minimization of the mean squared error (MSE) between the predicted output (a) and the actual target output (t), as described in (13).

$$P = \frac{1}{N}\sum_{v=1}^{N}(t_v - a_v)^2 \tag{13}$$

Where *N* represents the number of training samples, t_v is the desired output for the v[th] sample, and a_v is the predicted output. The training goal is to minimize this error across the dataset, thereby enabling the ANN to learn the optimal duty ratio for any given environmental condition.

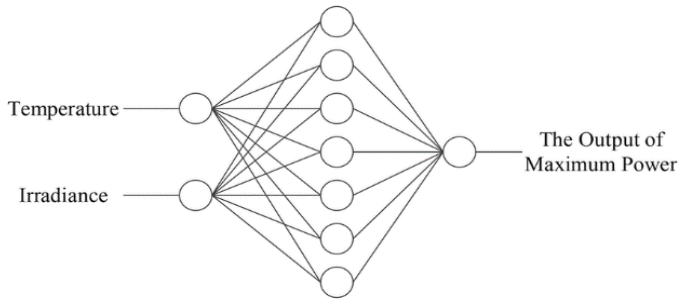

Figure 7. ANN-controlled MPPT structure [9]

The practical realization of ANN-based MPPT has been explored across various converter topologies, including Boost and CUK converters, where the ANN serves as an intelligent controller that continuously adjusts the operating point of the PV system. The simulation environment of MATLAB/Simulink was used to validate the model, confirming its superiority in both response time and tracking accuracy. Of particular interest is the use of feed-forward multi-layer neural networks, which consist of input, hidden, and output layers arranged in a forward-only topology. These architectures are capable of approximating highly nonlinear functions and can generalize well to unseen data, making them highly suitable for real-world solar energy systems that encounter varying operational conditions throughout the day. Intrinsically, ANN-controlled MPPT represents a paradigm shift in PV energy optimization moving from rule-based logic to intelligent, self-adaptive systems. By learning from data and continuously evolving, ANN-driven controllers not only enhance energy harvesting efficiency but also pave the way for next-generation smart PV grids capable of operating autonomously and optimally under diverse and dynamic conditions [31].

3.4. Fuzzy logic controller MPPT

The emergence of fuzzy logic as a robust method for handling uncertainty in complex systems can be credited to Lotfi Zadeh, whose pioneering work laid the foundation for fuzzy set theory. In the realm of photovoltaic (PV) systems, this approach has translated into the development of the fuzzy logic controller (FLC), a nonlinear, rule-based control method that effectively integrates expert knowledge and heuristic decision-making into the control algorithm. Unlike traditional MPPT techniques that rely heavily on linear models and mathematical precision, FLCs thrive in uncertain, nonlinear, and rapidly changing environments, making them particularly well-suited for solar power applications. At its core, the FLC for MPPT comprises four main components: fuzzification, fuzzy rule base, inference mechanism, and defuzzification. Each plays a critical role in enabling the controller to dynamically determine the optimal duty cycle adjustment for a DC-DC converter, thus allowing the PV system to operate at or near the maximum power point (MPP) under varying solar and environmental conditions [23].

a) Fuzzification

The fuzzification process translates crisp numerical inputs into linguistic fuzzy variables. In the proposed controller, the two primary inputs are the error (e) and the change in error (ce), calculated at each sampling instant (k). These are defined mathematically in (14) and (15).

$$e\ (k) = \frac{P(k)-P(k-1)}{I(k)-I(k-1)} \quad (14)$$

$$ce\ (k) = e(k) - e(k-1) \quad (15)$$

Here, *P(k)* represents the instantaneous power of the PV array, and *I(k)* its corresponding current. These inputs are then mapped to linguistic subsets, negative big (NB), negative small (NS), zero (Z0), positive small (PS), and positive big (PB), through membership functions. These functions graphically define the degree of belonging for each input variable to its corresponding fuzzy set, enabling the controller to

interpret the inputs in qualitative terms. Figure 8 illustrates the membership functions for the input variables and the output (duty cycle change, ΔD).

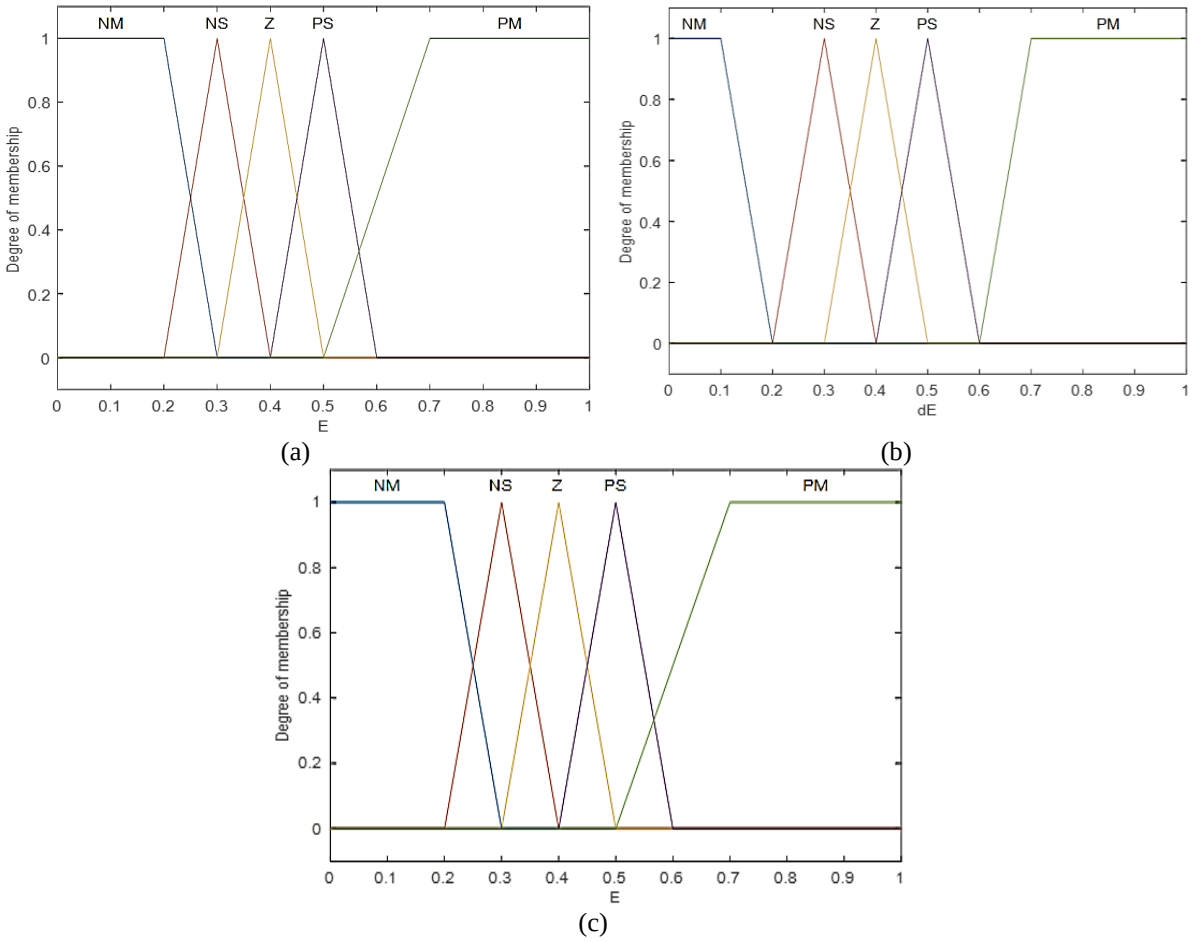

Figure 8. Defined membership functions: (a) converter input current, (b) converter input voltage, and (c) fuzzy controller output duty cycle

b) Fuzzy rule base

The fuzzy rule base acts as the brain of the controller, comprising a collection of IF-THEN rules that encapsulate expert knowledge and intuitive control responses. These rules relate the fuzzy inputs to corresponding fuzzy outputs and allow the system to react intelligently to varying conditions. The fuzzy logic system is thus capable of mimicking human-like decision-making, adjusting the converter behavior based on prior experience and system knowledge [23].

c) Inference mechanism

Inference is the reasoning engine of the FLC. It interprets the rule base by evaluating the fuzzy inputs and determining how each rule should be applied. The output fuzzy sets are combined using methods such as Mamdani or Takagi-Sugeno-Kang (TSK) inference. Mamdani inference, for example, is known for its intuitive and interpretable rule representation, while TSK is computationally more efficient for real-time applications. The selected inference method synthesizes the various rule outcomes into a composite fuzzy output representing the overall control action [23].

d) Defuzzification

The final stage in the fuzzy control loop is defuzzification, which converts the aggregated fuzzy output back into a crisp control signal that can be implemented by the DC-DC converter. Among various defuzzification methods, the center of gravity (COG) and center of area (COA) are most commonly used due to their balanced representation of fuzzy sets. In this study, the output (ΔD(k) is computed using the weighted average of the membership values, as shown in (16) and (17).

$$\Delta D(k) = \frac{\sum_{v-1}^{n} \mu(\Delta D_v(k)) \times \Delta D_v(k)}{\sum_{v-1}^{n} \mu(\Delta D_v(k))} \quad (16)$$

$$\Delta D(k) = D(k-1) + \Delta D(k) \quad (17)$$

The resulting duty ratio (D(k)) then determines the converter's switching behavior, effectively adjusting the operating point of the PV system to track the MPP. To evaluate the controller's performance, a MATLAB/Simulink model was developed, depicted in Figure 9, incorporating dynamic changes in solar irradiation from 200 W/m² to 1000 W/m². The results demonstrate that the FLC-based MPPT exhibits strong adaptability and consistent performance across varying conditions. Unlike conventional MPPT algorithms, which may falter under transient conditions or require intricate tuning, the FLC adapts quickly and reliably without the need for a precise mathematical model of the PV system. The FLC-based MPPT algorithm stands out for its flexibility, simplicity, and real-world applicability. It bridges the gap between model-based and heuristic control by embedding intuitive knowledge into a formal decision-making framework. This makes it an attractive solution for grid-tied PV systems operating under diverse and unpredictable environmental conditions.

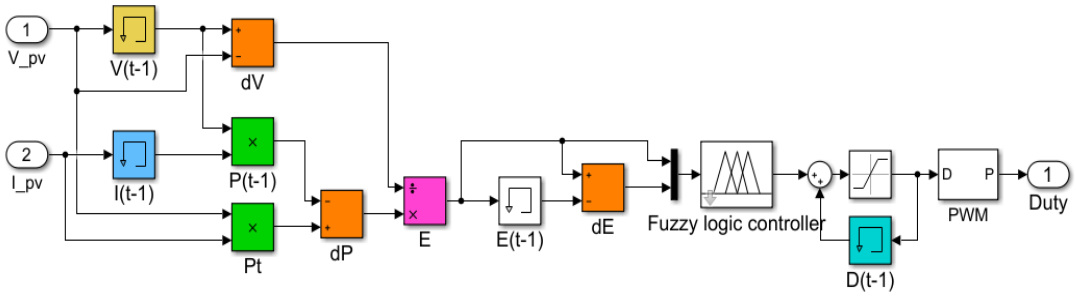

Figure 9. FLC-based MPPT Simulink model

4. RESULTS AND DISCUSSION

To evaluate the performance of different MPPT algorithms, simulations were conducted under varying irradiance and temperature conditions. The algorithms assessed include perturb and observe (P&O), incremental conductance (InC), artificial neural network (ANN)-based MPPT, and fuzzy logic controller (FLC)-based MPPT. The primary metrics for comparison were tracking efficiency, response time, and stability under dynamic environmental conditions. Figure 10 presents the comparative power outputs of the four MPPT algorithms under simulated dynamic irradiance conditions. The P&O algorithm, shown in red, exhibited the lowest steady-state power output due to its inherent oscillations around the maximum power point. The InC method, represented in orange, showed improved performance with relatively smoother tracking and better average power output compared to P&O. The FLC, in yellow, demonstrated the highest and most stable power output throughout the simulation, with an output of 1.019×10^6 W. The FLC's power indicates an effective and accurate MPPT tracking. The artificial neural network (ANN)-based MPPT, represented in purple, closely followed the FLC in terms of output power but showed slight oscillatory behavior, especially in the early stages of convergence. These results highlight the superior performance of intelligent control techniques, particularly FLC and ANN, over conventional methods. The FLC-based MPPT consistently maintained peak power, underscoring its adaptability and precision in handling non-linear PV characteristics.

Figure 10 illustrates the dynamic performance comparison of four MPPT algorithms, P&O, InC, ANN, and FLC under simulated irradiance conditions. Notably, both the ANN and FLC algorithms demonstrate superior power output characteristics, each reaching a peak magnitude of approximately 1.098×10^6 W. At around 0.01 seconds, all algorithms exhibit a sharp power rise, converging toward their respective maximum points. However, both ANN and FLC respond more rapidly and effectively, attaining the maximum perturbation point at 0.034 seconds, where their power values temporarily align with those of the conventional P&O and InC methods. Beyond this point, a divergence in performance becomes evident. The FLC-based MPPT outperforms all others by maintaining a consistently higher output—approximately 1.019×10^6 W with minimal oscillation, stabilizing much earlier at around 0.16 seconds. In contrast, while the ANN-based MPPT tracks closely behind, it exhibits slightly higher perturbation and oscillation before stabilizing, indicating a marginally slower convergence to steady-state compared to FLC.

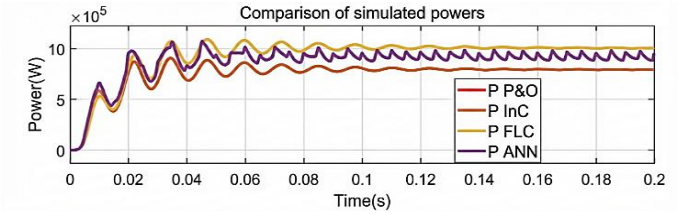

Figure 10. MPPT power settling comparison

On the other hand, the traditional P&O and InC methods yield noticeably lower power levels throughout the simulation, stabilizing at about 1.098×10^4 W after 0.16 seconds. These methods show slower response times and larger steady-state errors, highlighting their limitations in rapidly changing irradiance conditions. The simulation results reinforce the effectiveness of intelligent MPPT algorithms, particularly FLC, which offers the best combination of accuracy, speed, and stability in MPP tracking. The ANN algorithm also demonstrates high potential, albeit with a slightly delayed settling time, while P&O and InC are more susceptible to performance degradation under dynamic operating conditions.

Figure 11 presents a comparative analysis of the simulated voltage responses for the four MPPT algorithms. Initially, all algorithms exhibit a rapid voltage rise, with the first notable perturbation occurring around 0.01 seconds, marking the onset of the Maximum Power Point Tracking (MPPT) process. During this early transient phase, the P&O, InC, and ANN algorithms momentarily surpass the FLC in reaching their peak voltage values, indicating faster initial response in terms of voltage rise. However, as the simulation progresses, a shift in performance emerges. By approximately 0.0346 seconds, the FLC-based algorithm overtakes the others and begins to exhibit superior voltage regulation. It not only reaches a higher steady-state voltage compared to its counterparts but also demonstrates enhanced damping characteristics, as evidenced by the reduced amplitude of voltage oscillations and quicker settling time. This highlights the FLC algorithm's robustness in handling dynamic changes while maintaining voltage stability.

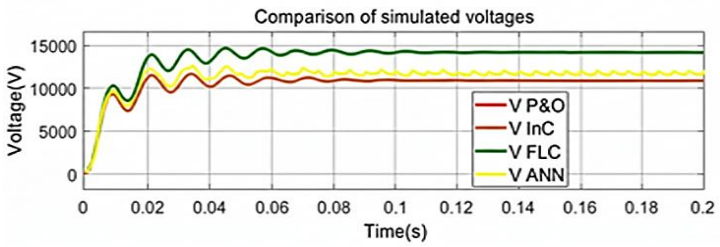

Figure 11. Plot of different algorithms' voltages under constant states

The P&O and InC algorithms converge to similar steady-state voltages but at a lower magnitude than FLC, and they also display persistent oscillations, which reflect their slower adaptation and sensitivity to perturbations in environmental conditions. The ANN algorithm, although initially faster, lags behind in stabilizing compared to FLC and shows a slightly lower final voltage level with minor fluctuations, which may be attributed to the complexity of training convergence and dependency on data quality. While conventional algorithms like P&O and InC perform adequately, their steady-state performance is outpaced by intelligent controllers. The FLC demonstrates the best voltage stability and regulation, followed by ANN, affirming the value of advanced control logic in PV system MPPT strategies. These results are particularly important for grid-tied PV systems, where voltage consistency is essential for safe and efficient operation.

The performance analysis of the MPPT algorithms under a solar irradiance of 600 W/m² and constant temperature, as presented in Figures 12 and 13, reveals significant insights into the dynamic and steady-state behavior of each algorithm within a grid-tied photovoltaic (PV) system. Figure 12, which illustrates the comparison of simulated power outputs, highlights key transition points where the behaviors of the FLC, ANN, P&O, and InC algorithms intersect or converge. At 0.14 seconds, the power output of the FLC algorithm experiences a noticeable decline, settling at 7.44×10^5 W. This drop results in the FLC power output equating to the nearly constant power levels maintained by both the P&O and InC algorithms. The point of convergence suggests that the previously dynamic response of the FLC method temporarily aligns with the more stable performance of the conventional algorithms. Shortly after, at 0.15 seconds, the ANN

algorithm, undergoing a gradual decline in its power output, also matches the power level of P&O and InC at 7.44×10^5 W.

This again demonstrates a transient convergence point, signifying that ANN, despite its adaptive capabilities, can briefly synchronize with conventional algorithms during certain system transitions. Finally, at 0.185 seconds, the power outputs of all four algorithms converge at 4.045×10^5 W, a steady-state value that likely reflects the system's stabilization under the constant irradiance condition. This convergence suggests that, regardless of the differences in algorithmic complexity and adaptability, the system eventually reaches a uniform operating point.

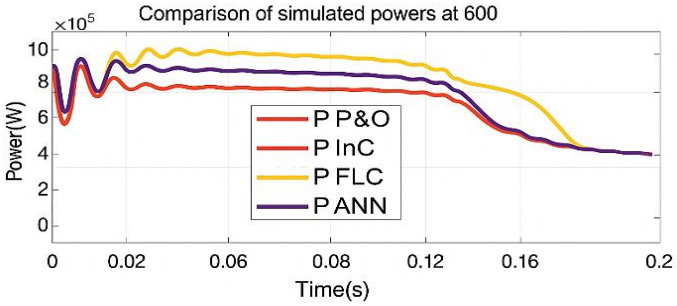

Figure 12. Plot of different algorithms' powers at 600 W/m^2 with constant temperature

In Figure 13, which displays the comparison of simulated voltage responses of the same algorithms, a similarly insightful trend is observed. At 0.0346 seconds, the FLC algorithm exhibits a higher voltage output than its counterparts, with P&O, InC, and ANN all outputting 1.474×10^4 V. This early superiority in voltage response indicates the FLC's quick adaptability and rapid tracking behavior, which is a direct result of its rule-based decision-making logic that enables it to respond efficiently to input changes. As time progresses, at 0.145 seconds, the voltage output of FLC, during its downward trend, matches the voltage values of the other algorithms, P&O, InC, and ANN each around 10,000 V.

This moment of equality illustrates another transient phase where both adaptive and heuristic algorithms reach similar performance levels before diverging again. At 0.18 seconds, P&O and InC show greater voltage stability by maintaining a constant output of 9700 V, while ANN continues its downward slope and records a slightly lower voltage of 9500 V.

The observed behavior suggests that traditional algorithms like P&O and InC offer steadier voltage regulation than ANN, which may require additional tuning to maintain performance under stable environmental conditions. Interestingly, by 0.19 seconds, P&O, InC, and ANN all align with a voltage value of 9500 V, while the FLC algorithm displays a slightly improved output of 9700 V. This demonstrates the FLC's capacity to recover and maintain higher voltage output compared to the others, even after a decline phase.

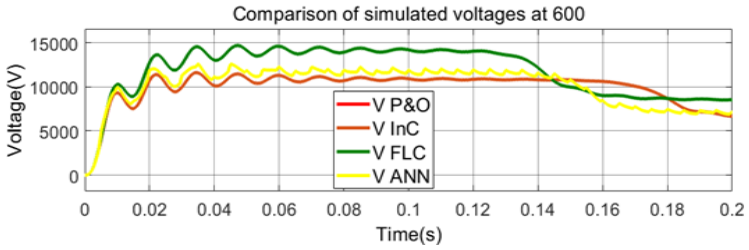

Figure 13. Plot of different algorithms' voltages at 600 W/m^2 with constant temperature

The comparative analysis underlines the strengths and limitations of each algorithm. The FLC method is shown to be highly responsive and adaptive during transients, although it may experience temporary instability. ANN also exhibits adaptive learning capabilities but tends to require more time to converge towards stability, especially in constant conditions. On the other hand, P&O and InC prove to be more consistent and stable in both power and voltage outputs, making them reliable choices for scenarios where simplicity and steady operation are preferred. Nevertheless, the brief points of convergence and

divergence among all the algorithms indicate that no single method is universally optimal across all operating conditions. Therefore, combining the fast-tracking abilities of FLC, the intelligent adaptation of ANN, and the stability of conventional techniques like P&O and InC may offer a more robust and efficient MPPT control strategy for grid-connected PV systems.

The results illustrated in Figures 14 and 15 highlight the performance of the four MPPT algorithms under a steady irradiance condition and an increased ambient temperature of 30°C. These figures demonstrate that, despite the temperature rise, both power and voltage outputs across all algorithms remain largely stable throughout the simulation. However, a closer inspection reveals that the FLC algorithm consistently outperforms the others in both power and voltage regulation.

In Figure 14, the power outputs of all algorithms initially exhibit transient oscillations as they converge toward their respective steady-state operating points. After approximately 0.1 seconds, the outputs stabilize. While the P&O and InC algorithms show moderate power output and relatively slower settling behavior, the ANN and FLC algorithms demonstrate faster convergence and smoother profiles. Among them, the FLC algorithm achieves the highest and most stable power output, indicating superior tracking efficiency and a quicker ability to lock onto the maximum power point under the given conditions. This advantage becomes particularly important in real-world applications where rapid adaptation and minimal power loss are crucial.

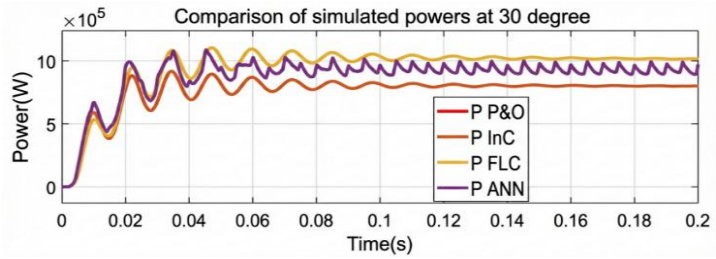

Figure 14. Plot of different algorithms' power at 30 °C with constant irradiance

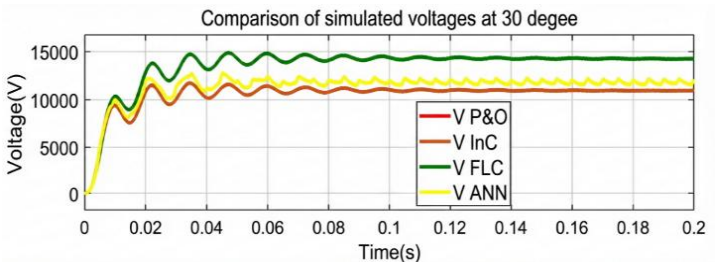

Figure 15. Plot of different algorithms' voltage at 30 °C with constant irradiance

Figure 15 further reinforces the dominance of the FLC approach. The voltage outputs of all algorithms again show brief fluctuations early on, followed by stabilization. The FLC algorithm not only reaches its steady-state voltage faster than the others but also maintains the highest voltage level throughout the simulation period. This is a clear indication of its robustness and effectiveness in extracting the maximum energy from the PV system under elevated temperature conditions. While the ANN also performs well and shows a relatively high and stable voltage output, it still falls slightly behind the FLC. In contrast, the P&O and InC methods maintain lower, though stable, voltage outputs, reflecting their simpler logic and less adaptive nature. The findings from Figures 14 and 15 confirm that the FLC algorithm exhibits superior performance in both dynamic response and steady-state behavior, making it the most effective among the four algorithms evaluated. It not only responds quickly to environmental conditions but also sustains higher power and voltage outputs consistently. The ANN algorithm shows promise with its learning-based adaptability, but remains slightly behind the FLC in steady-state values. Conventional algorithms like P&O and InC offer reliable performance but are clearly outperformed in both responsiveness and output efficiency. These results emphasize the potential of FLC-based MPPT for optimized operation in grid-tied photovoltaic systems, particularly under fluctuating environmental conditions such as temperature variations.

The performance of the four MPPT algorithms was evaluated under both standard test conditions (STC) and dynamic scenarios involving irradiance fluctuations, as illustrated in Figures 10 and 11 and summarized in Tables 3 and 4. Under STC (1000 W/m², 25 °C), Table 3 shows that both P&O and InC techniques converged to the same operating point at time t = 0.16 s, with identical input voltages of 3711 V and output voltages of 1.088×10^4 V, achieving an output power of 8.032×10^5 W. These results highlight the similarity in behavior of these conventional algorithms under steady-state conditions. On the other hand, the ANN-based MPPT showed better performance with an increased input voltage of 6283 V and a corresponding output voltage of 1.200×10^4 V, achieving a higher power output of 9.650×10^5 W. The FLC algorithm delivered the best results under these conditions, reaching an output voltage of 1.422×10^4 V and power of 1.019×10^6 W, confirming its superior tracking ability and quick convergence to the MPP.

This performance trend is further supported by Figure 10, where the FLC and ANN curves rise sharply and stabilize earlier compared to P&O and InC. The power generated by FLC and ANN exceeds that of the conventional algorithms throughout the simulation, with the FLC output peaking at 1.098×10^6 W and stabilizing faster around t = 0.16 s. Figure 11 shows similar behavior in terms of voltage tracking, where FLC again leads with the highest and most stable voltage curve, while P&O and InC exhibit persistent ripples and slower settling.

Under variable irradiance and constant temperature, the simulation mimicked real-world operating conditions where solar irradiance changes due to partial shading or cloud coverage. As shown in Table 4, P&O and InC still mirrored each other, with a drop in input voltage to 3566 V, and output power decreasing to 7.443×10^5 W at an irradiance level of 600 W/m². Their output voltages fell slightly to 1.058×10^4 V, indicating a proportional decline in performance due to reduced solar input. The ANN algorithm, however, maintained a relatively high input voltage of 6283 V and an output voltage of 1.174×10^4 V, yielding a robust power output of 8.930×10^5 W, demonstrating its adaptability to environmental changes. The FLC showed a more significant drop in output power to 4.040×10^5 W, possibly due to the fuzzy rules being less tuned for abrupt irradiance transitions, although it still outperformed conventional methods in terms of voltage stability with 4320 V input and 9048 V output.

The FLC-based MPPT algorithm, therefore, proves highly effective in both stable and variable irradiance conditions, showing resilience and precision in maintaining high power output and system voltage. FLC excels under constant conditions, while conventional algorithms like P&O and InC, though simpler, lag in both responsiveness and efficiency. These findings support the integration of intelligent control techniques for modern grid-tied PV systems where dynamic adaptation and maximum energy extraction are critical.

Table 3. Results under STC

Algorithm	Time (s)	Input voltage (V)	Output power (W)	Output voltage (V)
P&O	0.16	3711	8.032×10^5	1.088×10^4
InC	0.16	3711	8.032×10^5	1.088×10^4
ANN	0.16	6283	9.650×10^5	1.200×10^4
FLC	0.16	7084	1.019×10^6	1.422×10^4

Table 4. Different results under partial shading conditions, constant temperature, and variable irradiance

Algorithm	Time (s)	Input voltage (V)	Output power (W)	Output voltage (V)
P&O	0.16	3566	7.443×10^5	1.058×10^4
InC	0.16	3566	7.443×10^5	1.058×10^4
ANN	0.16	6283	8.930×10^5	1.174×10^4
FLC	0.16	4320	4.040×10^5	9048

5. CONCLUSION

This study presented a comprehensive comparative assessment of four Maximum Power Point Tracking (MPPT) algorithms, perturb and observe (P&O), incremental conductance (InC), fuzzy logic controller (FLC), and artificial neural network (ANN), for a grid-tied photovoltaic (PV) system under both standard test conditions (STC) and dynamically varying irradiance scenarios. Simulations were carried out using MATLAB/Simulink, with a boost converter integrated to emulate realistic power conversion behavior. Under STC, both P&O and InC achieved equivalent performance, with a peak output power of 8.032×10^5 W and an output voltage of 1.088×10^4 V, confirming their adequacy under stable environmental conditions. However, intelligent controllers demonstrated superior performance: FLC achieved the highest power output of 1.019×10^6 W with a corresponding voltage of 1.422×10^4 V, while the ANN algorithm followed closely with 9.650×10^5 W and 1.200×10^4 V, respectively.

When subjected to partial shading and variable irradiance, performance deviations became more pronounced. The ANN-based approach showed excellent adaptability to environmental fluctuations, maintaining a high and stable output of 8.930×10^5 W at 1.174×10^4 V, illustrating strong robustness and rapid dynamic response. By contrast, P&O and InC saw a significant reduction in performance, with outputs dropping to 7.443×10^5 W, emphasizing their sensitivity to non-uniform conditions. FLC, while outperforming conventional methods under uniform conditions, showed limited adaptability under dynamic conditions, with output power declining to 4.040×10^5 W. These results reinforce the potential of intelligent MPPT strategies in modern PV systems. Among the tested algorithms, ANN consistently exhibited the best balance of tracking speed, voltage stability, and robustness to varying irradiance levels. FLC also demonstrated competitive advantages, particularly in scenarios with imprecise or nonlinear system characteristics due to its model-free nature and inherent fault tolerance. Beyond algorithmic performance, this work aligns with the global shift toward cleaner energy alternatives, driven by environmental and economic imperatives. By demonstrating how advanced MPPT techniques can efficiently extract up to 775 kW of solar power, this research underscores the importance of adaptive and intelligent controllers in improving the reliability and performance of grid-tied PV systems.

Future research would prioritize the experimental validation of ANN and FLC algorithms in real-time hardware platforms, along with the development of hybrid MPPT techniques that fuse the complementary strengths of AI-based models and rule-based systems. Also, the integration of modern optimization and deep learning approaches could further enhance MPPT precision and dynamic responsiveness, particularly under complex and rapidly changing operating environments.

ACKNOWLEDGMENTS

This section should acknowledge individuals who provided personal assistance to the work but do not meet the criteria for authorship, detailing their contributions. It is imperative to obtain consent from all individuals listed in the acknowledgments.

FUNDING INFORMATION

The authors state that no external funding is involved in the study.

AUTHOR CONTRIBUTIONS STATEMENT

This journal uses the Contributor Roles Taxonomy (CRediT) to recognize individual author contributions, reduce authorship disputes, and facilitate collaboration.

Name of Author	C	M	So	Va	Fo	I	R	D	O	E	Vi	Su	P	Fu
Louis Nicase Nguefack	✓	✓	✓	✓		✓		✓	✓		✓			
Kayode Timothy Akindeji	✓			✓						✓	✓	✓		✓
Abayomi A. Adebiyi	✓	✓		✓	✓					✓	✓	✓	✓	

C : **C**onceptualization
M : **M**ethodology
So : **So**ftware
Va : **Va**lidation
Fo : **Fo**rmal analysis
I : **I**nvestigation
R : **R**esources
D : **D**ata Curation
O : Writing - **O**riginal Draft
E : Writing - Review & **E**diting
Vi : **Vi**sualization
Su : **Su**pervision
P : **P**roject administration
Fu : **Fu**nding acquisition

CONFLICT OF INTEREST STATEMENT

The authors state there is no conflict of interest.

DATA AVAILABILITY

The data supporting the findings of this study are available from the corresponding author, [AAA], upon reasonable request.

REFERENCES

[1] L. N. Nguefack, I. E. Davidson, and A. A. Adebiyi, "Maximum power point tracking algorithms performance comparison for a grid-tied photovoltaic system," in *2023 31st Southern African Universities Power Engineering Conference (SAUPEC)*, Jan. 2023, pp. 1–6. doi: 10.1109/SAUPEC57889.2023.10057945.

[2] B. Tyagi *et al*., "Global perspectives on rooftop solar energy: a deep dive on how leading economies advance rooftop solar energy adoption," no. September, 2024.

[3] C. L. Nkashama, "Maximum power point tracking algorithm for photovoltaic home power supply," 2011.

[4] A. A. Adebiyi and K. Moloi, "Renewable energy source utilization progress in South Africa: a review," *Energies*, vol. 17, no. 14, p. 3487, Jul. 2024, doi: 10.3390/en17143487.

[5] A. Shrivastava, R. Sharma, M. Kumar Saxena, V. Shanmugasundaram, M. Lal Rinawa, and Ankit, "Solar energy capacity assessment and performance evaluation of a standalone PV system using PVSYST," *Materials Today: Proceedings*, vol. 80, pp. 3385–3392, 2023, doi: 10.1016/j.matpr.2021.07.258.

[6] H. Tao, M. Ghahremani, F. W. Ahmed, W. Jing, M. S. Nazir, and K. Ohshima, "A novel MPPT controller in PV systems with hybrid whale optimization-PS algorithm based ANFIS under different conditions," *Control Engineering Practice*, vol. 112, p. 104809, Jul. 2021, doi: 10.1016/j.conengprac.2021.104809.

[7] U. Yilmaz, A. Kircay, and S. Borekci, "PV system fuzzy logic MPPT method and PI control as a charge controller," *Renewable and Sustainable Energy Reviews*, vol. 81, pp. 994–1001, Jan. 2018, doi: 10.1016/j.rser.2017.08.048.

[8] M. L. Katche, A. B. Makokha, S. O. Zachary, and M. S. Adaramola, "A Comprehensive review of maximum power point tracking (MPPT) techniques used in solar PV systems," *Energies*, vol. 16, no. 5, p. 2206, Feb. 2023, doi: 10.3390/en16052206.

[9] A. I. M. Ali and H. R. A. Mohamed, "Improved P&O MPPT algorithm with efficient open-circuit voltage estimation for two-stage grid-integrated PV system under realistic solar radiation," *International Journal of Electrical Power & Energy Systems*, vol. 137, p. 107805, May 2022, doi: 10.1016/j.ijepes.2021.107805.

[10] A. K. Sharma *et al.*, "Role of metaheuristic approaches for implementation of integrated MPPT-PV systems: a comprehensive study," *Mathematics*, vol. 11, no. 2, p. 269, Jan. 2023, doi: 10.3390/math11020269.

[11] A. Benlafkih, Y. El Moujahid, A. Hadjoudja, N. El Harfaoui, E.-B. Said, and M. C. El Idrissi, "Optimizing photovoltaic systems performance under partial shading using an advanced cuckoo search algorithm," *International Journal of Power Electronics and Drive Systems (IJPEDS)*, vol. 15, no. 2, p. 845, Jun. 2024, doi: 10.11591/ijpeds.v15.i2.pp845-857.

[12] N. Hashim and Z. Salam, "Critical evaluation of soft computing methods for maximum power point tracking algorithms of photovoltaic systems," *International Journal of Power Electronics and Drive Systems (IJPEDS)*, vol. 10, no. 1, p. 548, Mar. 2019, doi: 10.11591/ijpeds.v10.i1.pp548-561.

[13] M. Hamza Zafar *et al.*, "A novel meta-heuristic optimization algorithm based MPPT control technique for PV systems under complex partial shading condition," *Sustainable Energy Technologies and Assessments*, vol. 47, p. 101367, Oct. 2021, doi: 10.1016/j.seta.2021.101367.

[14] A. Behera and P. Mohanty, "A comparative study on grid-tied PV system using PV syst software & MATLAB," in *2024 IEEE Third International Conference on Power Electronics, Intelligent Control and Energy Systems (ICPEICES)*, Apr. 2024, pp. 526–531. doi: 10.1109/ICPEICES62430.2024.10719096.

[15] Z. Al Dodaev, T. Aziz, M. S. Rahman, and T. A. Joy, "Comparative analysis of the MPPT algorithm in a residence and a grid-connected solar PV system Under Partial Shade Conditions - A Review," *Control Systems and Optimization Letters*, vol. 2, no. 1, pp. 135–143, Jun. 2024, doi: 10.59247/csol.v2i1.91.

[16] S. Marlin and S. Jebaseelan, "A comprehensive comparative study on intelligence based optimization algorithms used for maximum power tracking in grid-PV systems," *Sustainable Computing: Informatics and Systems*, vol. 41, p. 100946, Jan. 2024, doi: 10.1016/j.suscom.2023.100946.

[17] S. A. Sarang *et al.*, "Maximizing solar power generation through conventional and digital MPPT techniques: a comparative analysis," *Scientific Reports*, vol. 14, no. 1, p. 8944, Apr. 2024, doi: 10.1038/s41598-024-59776-z.

[18] M. Shehab, F. B. Shannaq, H. Al-Aqrabi, and M. S. Daoud, "Enhancing chimp optimization algorithm using local search capabilities and machine learning for real engineering problems," *International Journal of Intelligent Engineering and Systems*, vol. 17, no. 5, pp. 538–552, 2024, doi: 10.22266/ijies2024.1031.42.

[19] M. Fathi and J. A. Parian, "Intelligent MPPT for photovoltaic panels using a novel fuzzy logic and artificial neural networks based on evolutionary algorithms," *Energy Reports*, vol. 7, pp. 1338–1348, Nov. 2021, doi: 10.1016/j.egyr.2021.02.051.

[20] Z. Chen *et al.*, "Rapid and accurate modeling of PV modules based on extreme learning machine and large datasets of I-V curves," *Applied Energy*, vol. 292, p. 116929, Jun. 2021, doi: 10.1016/j.apenergy.2021.116929.

[21] M. Dehghani, M. Taghipour, G. B. Gharehpetian, and M. Abedi, "Optimized fuzzy controller for MPPT of grid-connected PV systems in rapidly changing atmospheric conditions," *Journal of Modern Power Systems and Clean Energy*, vol. 9, no. 2, pp. 376–383, 2021, doi: 10.35833/MPCE.2019.000086.

[22] S. Chahar and D. K. Yadav, "Retrospection and investigation of ANN-based MPPT technique in comparison with soft computing-based MPPT techniques for PV solar and wind energy generation system," *International Journal of Mathematical Modelling and Numerical Optimisation*, vol. 14, no. 1/2, pp. 69–83, 2024, doi: 10.1504/IJMMNO.2024.143230.

[23] N. Zhani and H. Mahmoudi, "Comparison of the performance of MPPT control techniques (fuzzy logic, incremental conductance and perturb & observe) under MATLAB/Simulink," *IFAC-PapersOnLine*, vol. 58, no. 13, pp. 617–623, 2024, doi: 10.1016/j.ifacol.2024.07.551.

[24] B. Yang *et al.*, "Comprehensive overview of maximum power point tracking algorithms of PV systems under partial shading condition," *Journal of Cleaner Production*, vol. 268, p. 121983, Sep. 2020, doi: 10.1016/j.jclepro.2020.121983.

[25] M. E. Girgis and N. A. Elkhateeb, "Enhancing photovoltaic MPPT with P&O algorithm performance based on adaptive PID control using exponential forgetting recursive least squares method," *Renewable Energy*, vol. 237, p. 121801, Dec. 2024, doi: 10.1016/j.renene.2024.121801.

[26] M. S. Endiz, G. Gökkuş, A. E. Coşgun, and H. Demir, "A review of traditional and advanced MPPT approaches for PV systems under uniformly insolation and partially shaded conditions," *Applied Sciences*, vol. 15, no. 3, p. 1031, Jan. 2025, doi: 10.3390/app15031031.

[27] A. Chellakhi, S. El Beid, Y. Abouelmahjoub, and H. Doubabi, "An enhanced incremental conductance MPPT approach for PV power optimization: a simulation and experimental study," *Arabian Journal for Science and Engineering*, vol. 49, no. 12, pp. 16045–16064, Dec. 2024, doi: 10.1007/s13369-024-08804-1.

[28] M. S. Endiz, "Design and implementation of microcontroller-based solar charge controller using modified incremental conductance MPPT algorithm," *Journal of Radiation Research and Applied Sciences*, vol. 17, no. 2, p. 100938, Jun. 2024, doi: 10.1016/j.jrras.2024.100938.

[29] I. Al-Wesabi, Z. Fang, H. M. Hussein Farh, A. A. Al-Shamma'a, and A. M. Al-Shaalan, "Comprehensive comparisons of improved incremental conductance with the state-of-the-art MPPT Techniques for extracting global peak and regulating dc-link voltage," *Energy Reports*, vol. 11, pp. 1590–1610, Jun. 2024, doi: 10.1016/j.egyr.2024.01.020.
[30] S. Gul, S. M. Malik, Y. Sun, and F. Alsaif, "An artificial neural network based MPPT control of modified flyback converter for PV systems in active buildings," *Energy Reports*, vol. 12, pp. 2865–2872, Dec. 2024, doi: 10.1016/j.egyr.2024.08.082.
[31] S. R. Kiran, C. H. H. Basha, V. P. Singh, C. Dhanamjayulu, B. R. Prusty, and B. Khan, "Reduced simulative performance analysis of variable step size ANN based MPPT techniques for partially shaded solar PV systems," *IEEE Access*, vol. 10, pp. 48875–48889, 2022, doi: 10.1109/ACCESS.2022.3172322.

BIOGRAPHIES OF AUTHORS

Louis Nicase Nguefack is a Ph.D. student in the Department of Electrical Power Engineering at the Durban University of Technology (DUT), Durban, South Africa. He received his National Diploma from Mangosuthu University of Technology (MUT), Umlazi, South Africa 2017, B.Tech. and M.Eng. degrees in electrical engineering from Durban University of Technology (DUT) in 2019 and 2024, respectively. His research interests include renewable energy, smart grid, power electronics, artificial intelligence, and intelligent control. He can be contacted at email: 21434062@dut4life.ac.za.

Kayode Timothy Akindeji is currently an associate professor at the Department of Electrical Power Engineering, Durban University of Technology (DUT), Durban, South Africa, where he is also the acting head of department. He obtained his Ph.D. (electrical engineering) from the University of Kwa-Zulu Natal (UKZN), Durban, South Africa, in 2022. He is a registered professional engineering technologist (Pr Tech Eng) and a certified energy manager (C.E.M). His research interests include smart grids, renewable energy, distributed generation, energy management, energy efficiency, smart grid, and microgrid. He can be contacted at email: kayodea@dut.ac.za.

Abayomi A. Adebiyi is a senior lecturer in the Department of Electrical Power Engineering at the Durban University of Technology (DUT), Durban, South Africa. He got his doctorate degree in electrical engineering at the Durban University of Technology in 2021. His current research interests include power systems, power quality, renewable energy, grid optimization, and PV systems. He has published more papers in reputable Scopus-indexed journals in the fields of power systems and their applications. He can be contacted at email: abayomia@dut.ac.za.